Detecting and estimating signals in noisy cable structures: I. Neuronal noise sources

Amit Manwani [†] and Christof Koch [♯*]
Computation and Neural Systems Program,
California Institute of Technology, Pasadena, CA 91125.
[†] *quixote@klab.caltech.edu*, [♯] *koch@klab.caltech.edu*

[*]Author to whom correspondence should be addressed.

Abstract

In recent theoretical approaches addressing the problem of neural coding, tools from statistical estimation and information theory have been applied to quantify the ability of neurons to transmit information through their spike outputs. These techniques, though fairly general, ignore the specific nature of neuronal processing in terms of its known biophysical properties. However, a systematic study of processing at various stages in a biophysically faithful model of a single neuron can identify the role of each stage in information transfer. Towards this end, we carry out a theoretical analysis of the information loss of a synaptic signal propagating along a linear, one-dimensional, weakly-active cable due to the presence of neuronal noise sources distributed along its length, using both a signal reconstruction and a signal detection paradigm. Here we begin such an analysis by quantitatively characterizing three sources of membrane current noise. 1. Thermal noise due to the passive membrane resistance, 2. noise due to stochastic channel openings and closings of voltage-gated membrane channels (Na^+ and K^+), and 3. noise due to random, background synaptic activity. Using analytical expressions for the power spectral densities of these noise sources, we compare their magnitudes in the case of a patch of membrane from a cortical pyramidal cell and explore their dependence on different biophysical parameters.

1 Introduction

A great deal of effort in cellular biophysics and neurophysiology has concentrated on characterizing nerve cells as input-output devices. A host of experimental techniques like voltage clamp, current clamp, whole-cell recordings, and so on, have been used to study how neurons transform their synaptic inputs (which are in the form of conductance changes) to their outputs (usually in the form of a train of action potentials). It has been firmly established by now that neurons are highly sophisticated entities, potentially capable of implementing a rich panoply of powerful non-linear computational primitives (Koch, 1999).

A systematic investigation of the efficacy of neurons as communication devices dates back to well over 40 years ago (MacKay & McCulloch, 1952). More recently, tools from statistical estimation and information theory have been used (Rieke *et al.*, 1997) to quantify the ability of neurons to transmit information about random inputs through their spike outputs. Bialek (Bialek *et al.*, 1991; Bialek & Rieke, 1992) pioneered the use of the "reconstruction technique" towards this end, based on Wiener's earlier work (Wiener, 1949). These techniques have successfully been applied to understand the nature of neural codes in peripheral sensory neurons in various biological neural systems (Rieke *et al.*, 1997). Theoretical investigations into this problem since have given rise to

better methods of assessing capacity of neural codes (Strong *et al.*, 1998; Gabbiani, 1996; Theunissen & Miller, 1991).

In all the above approaches, the nervous system is treated like a black-box and is characterized empirically by the collection of its input-output records. The techniques employed are fairly general and consequently ignore the specific nature of information processing in neurons. Much is known about how signals are transformed and processed at various stages in a neuron (Koch, 1999) and a systematic study of neuronal information processing should be able to identify the role of each stage in information transfer. One way to address this question is to pursue a reductionist approach and apply the above tools to the individual components of a neuronal link. This allows us to assess the role of different neuronal sub-components (*viz.,* the synapse, the dendritic tree, the soma, the spike initiation zone and the axon) in information transfer from one neuron to another.

Using this approach, we can address critical questions such as, which stage represents a bottle-neck in information transfer, are the different stages matched to each other in order to maximize the amount of information transmitted, how does neuronal information processing depend on the different biophysical parameters which characterize neuronal hardware and so on. Thus, the rewards from such a biophysical approach to studying neural coding are multifarious. However, first we need to characterize the different noise sources which cause information loss at each stage in neuronal processing. For the purposes of this paper (and its sequel), we focus on linear one-dimensional dendritic cables. An analysis of the information capacity of a simple model of a cortical synapse illustrating the generality our approach has already been reported(Manwani & Koch, 1998).

Here we begin such a theoretical analysis of the information loss experienced by a signal as it propagates along a one-dimensional cable structure due to different types of distributed neuronal noise sources (as discussed extensively in (DeFelice, 1981)). We consider two paradigms: *signal detection* in which the presence or absence of a signal is to be detected, and *signal estimation* in which an applied signal needs to be reconstructed. This calculus can be regarded as a model for electrotonic propagation of synaptic signals to the soma along a linear, yet weakly-active dendrite.

For real neurons, propagation is never entirely linear; the well-documented presence of voltage-dependent membrane conductances in the dendritic tree can dramatically influence dendritic integration and propagation of information. Depending on their relative densities, the presence of different dendritic ion channel species can lead to both non-linear amplification of synaptic signals, combating the loss due to electrotonic attenuation (Bernander *et al.*, 1994; Stuart & Sakmann, 1994; Stuart & Sakmann, 1995; Cook & Johnston, 1997; Schwindt & Crill, 1995; Magee *et al.*, 1998) and a decrease in dendritic excitability or attenuation of synaptic signals (Hoffman *et al.*, 1997; Magee *et al.*, 1998; Stuart & Spruston, 1998).

The work discussed here is restricted to linear cables (passive or quasi-active (Koch, 1984); that is, the membrane can contain inductive-like components arising from time-dependent conductances) and can be regarded as a first order approximation to dendritic integration, which is amenable to closed-form analysis. Biophysically accurate scenarios which consider the effect of strong active non-linear membrane conductances can only be analyzed using numerical simulations and will be reported in the future.

Our efforts to date can be conveniently divided into two parts. In the first part, described in the present paper, we characterize three sources of noise which arise in nerve membranes: 1. thermal noise due to membrane resistance (*Johnson Noise*), 2. noise due to the stochastic channel openings and closings of two voltage-gated membrane channels, and 3. noise due to random background synaptic activity. Using analytical expressions for the power spectral densities of these noise sources, we compute their magnitudes for biophysically plausible parameter values obtained from different neuronal models in the literature.

In a second step, reported in the following paper, we carry out a theoretical analysis of the information loss of a synaptic signal as it propagates to the soma, due to the presence of these noise sources along the dendrite. We model the dendrite as a weakly-active linear cable with noise sources distributed all along its length and derive expressions for the capacity of this dendritic information channel under the signal detection and estima-

tion paradigms. We are also engaged in carrying out quantitative comparison of these noise estimates against experimental data (Manwani *et al.*, 1998).

A list of symbols used in the two papers is included in Appendix 1.

2 Sources of Neuronal Noise

In general, currents flowing through ion-specific membrane proteins (channels) depend non-linearly on the voltage difference across the membrane (Johnston & Wu, 1995),

$$i = f(V_m) \tag{1}$$

where i represents the ionic current through the channel and V_m is the membrane voltage. Often the current satisfies Ohm's law (Hille, 1992); i can be expressed as the product of the driving potential across the channel $V_m - E_{ch}$ and the voltage- (or ligand concentration) dependent channel conductance g_{ch} as,

$$i = g_{ch}(V_m)\,(V_m - E_{ch}) \tag{2}$$

where E_{ch} (the membrane voltage for which $i = 0$) is the reversal potential of the channel.

If i is small enough so that the flow of ions across the membrane does not significantly change V_m, the change in ionic concentrations is negligible (E_{ch} does not change) and so the driving potential is almost constant and $i \propto g_{ch}$. Thus, for a small conductance change, the channel current is approximately independent of V_m and is roughly proportional to the conductance change. Thus, even though neuronal inputs are usually in terms of conductance changes, for small inputs, currents can equivalently be regarded as the inputs. This argument holds for both ligand-gated and voltage-gated channels. We shall use this assumption throughout this paper and regard currents, and not conductances, as the input variables.

The neuron receives synaptic signals at numerous locations along its dendritic tree. These current inputs are integrated by the tree and they propagate as voltages towards the soma and the axon hillock, close to the site where the action potentials are generated. Thus, if we restrict ourselves to the study of the information loss due to the dendritic processing that precedes spike generation, currents are the input variables and the membrane voltage at the spike initiating zone can be considered to be the output variable.

We first consider some of the current noise sources present in nerve membranes which distort the synaptic signal as it propagates along the cable. As excellent background source text on noise in neurobiological systems, we recommend the monograph by DeFelice, (1981).

2.1 Thermal Noise

Electrical conductors are sources of thermal noise resulting from random thermal agitation of the electrical charges in the conductor. Thermal noise, also known as *Johnson noise*, represents a fundamental lower limit of noise in a system and can be reduced only by decreasing the temperature or the bandwidth of the system (Johnson, 1928). Thermal noise is also called *white noise* because its power spectral density is flat for all frequencies (except at very high frequencies where quantum effects come into play). Since thermal noise results from a large ensemble of independent sources, its amplitude distribution is Gaussian as dictated by the Central Limit Theorem (Papoulis, 1991). The power spectral density of the voltage fluctuations due to thermal noise (denoted by S_{Vth}) in a conductor of resistance R in equilibrium, (no current flowing through the conductor) is given by,

$$S_{Vth}(f) = 2kTR \quad \text{(units of V}^2\text{/Hz)}, \tag{3}$$

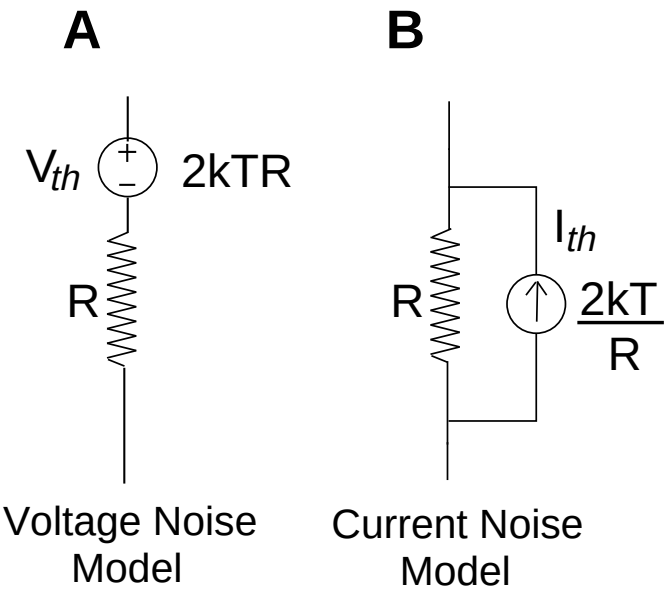

Figure 1: **Equivalent Thermal Noise Models for a Resistor.** Thermal noise due to a resistor R in thermal equilibrium at temperature T can be considered equivalently as **A** a voltage noise source V_{th} with power spectral density $2kTR$ in series with a noiseless resistance R or as **B** a current noise source I_{th} with power spectral density $2kT/R$ in parallel with a noiseless R.

where k denotes the Boltzmann constant and T is the absolute temperature of the conductor. Consequently, the variance of the voltage fluctuations due to thermal noise, σ^2_{Vth} is

$$\sigma^2_{Vth} = \int_{-B}^{B} S_{Vth}(f)\, df = 4kTRB \quad (\text{units of V}^2) \tag{4}$$

where B denotes the bandwidth of the measurement system.[1]

Thus, a conductor of resistance R can be replaced by an ideal noiseless resistor R in series with a voltage noise source $V_{th}(t)$, which has a power spectral density given by $S_{Vth}(f)$ (Figure 1A). Equivalently, one can replace the conductor with a noiseless resistor R in parallel with a current noise source, $I_{th}(t)$ with power spectral density denoted by $S_{Ith}(f)$ (Figure 1B) given by the expression,

$$S_{Ith}(f) = \frac{2kT}{R} \quad (\text{units of A}^2/\text{Hz}). \tag{5}$$

Since we assume the inputs to be currents, we shall use the latter representation. A passive one-dimensional cable can be modeled as a distributed network of resistances and capacitances as shown in Figure 2. r_m and c_m denote the resistance and the capacitance across the membrane (transversely) respectively. r_i represents the resistance (longitudinal) of the intra-cellular cytoplasm. c_m arises due to the capacitance of the thin, insulating, phospholipid bilayer membrane which separates the intra-cellular cytoplasm and external solution. In general, excitable membrane structures containing active voltage- and time- dependent conductances cannot be modeled as ladder networks consisting of resistances and capacitances alone, even if they behave linearly in a given voltage range. The time-dependent nature of voltage-gated channel conductances gives rise to *phenomenological* inductances (Sabah & Leibovic, 1969; Mauro *et al.*, 1970; Sabah & Leibovic, 1972; Mauro *et al.*, 1972; Koch, 1984). Thus, in general, the small-signal circuit equivalent of an active, linearized membrane is an RLC (resistor-inductor-capacitor) circuit consisting of resistances, capacitances and inductances. For an illustration of this

[1] All power spectral densities are assumed to be double-sided, since the power spectra of real signals are even functions of frequency.

linearization procedure, refer to the independent Appendix (*Small Signal Impedance of Active Membranes*) available over the Internet[2] or to Chapter 10 in Koch (1999).

However, when the time constants corresponding to the ionic currents are much smaller than the passive membrane time constant, the phenomenological inductances are negligible and the equivalent circuit reduces to the passive ladder model for cable. This is true for the case we consider, the passive membrane time constant is about an order of magnitude greater than the slowest time-scale of the noise sources and so the approximation above is a reasonable one. r_m reflects the effective resistance of the lipid bilayer (very high resistance) and the various voltage-gated, ligand-gated and leak channels embedded in the lipid matrix. Here we ignore the external resistance, r_e, of the external medium surrounding the membrane. All quantities (r_i, r_m, c_m) are expressed in per unit length of the membrane and have the dimensions of Ω/μm, $\Omega\ \mu m$ and F/μm respectively. For a linear cable, modeled as a cylinder of diameter d, $r_m = R_m/\pi\, d$, $c_m = \pi\, d\, C_m$, $r_i = 4R_i/\pi\, d^2$ where R_m, C_m and R_i (*specific membrane resistance* , *specific membrane capacitance* and *axial resistivity* respectively) are the usual biophysical parameters of choice.

The current noise due to r_m, has power spectral density,

$$S_{Ith}(f) = \frac{2kT}{r_m} \quad (\text{units of A}^2/\text{Hz } \mu\text{m})\,. \tag{6}$$

However, r_m is not the only source of thermal noise. The resistance r_i, representing the axial cytoplasmic resistance also contributes thermal noise. In general, the power spectral density of the voltage noise due to thermal fluctuations in an impedance Z is given by

$$S_{Vth}(f) = 2kT\,Re\{Z(f)\}\,, \tag{7}$$

where $Re\{Z(f)\}$ is the real part of the impedance as a function of frequency. Thus, the voltage variance is given by

$$\sigma^2_{Vth} = \int_{-\infty}^{\infty} S_{Vth}(f)\ df \quad (\text{units of V}^2)\,. \tag{8}$$

For an infinite passive cable (Figure 2), the input impedance is given as

$$Z(f) = \frac{\sqrt{r_i r_m}}{\sqrt{1 + j2\pi f\tau_m}} \tag{9}$$

$$\Rightarrow\ Re\{Z(f)\} = \frac{\sqrt{r_i r_m}}{[1 + (2\pi f\tau_m)^2\,]^{1/4}}\ \cos\left(\frac{\tan^{-1} 2\pi f\tau_m}{2}\right) \tag{10}$$

which yields

$$S_{Vth}(f) = \frac{2kT\sqrt{r_i r_m}}{[1 + (2\pi f\tau_m)^2\,]^{1/4}}\ \cos\left(\frac{\tan^{-1} 2\pi f\tau_m}{2}\right)\,. \tag{11}$$

The integral of $S_{Vth}(f)$ in the equation above is divergent, and so σ^2_{Vth} is infinite. This can be seen easily by rewriting the expression for S_{Vth} as

$$S_{Vth}(f) = \sqrt{2\, r_i r_m}\ kT\left[\frac{1}{1 + (2\pi f\tau_m)^2} + \frac{1}{\sqrt{1 + (2\pi f\tau_m)^2}}\right]^{1/2}\,. \tag{12}$$

[2]The postscript or pdf documents are available at `http://www.klab.caltech.edu/~quixote/publications.html`

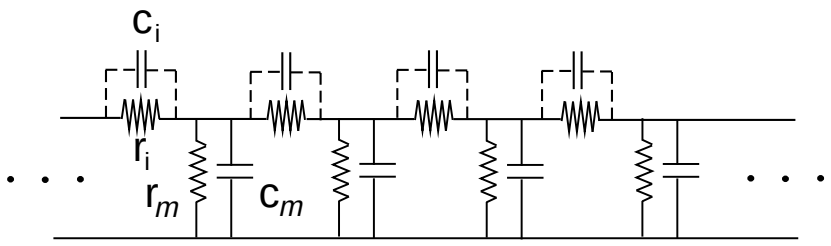

Figure 2: **Ladder Network Model of an Infinite 1-D Linear Cable.** r_i represents the longitudinal (axial) resistance due to the cytoplasm, whereas r_m and c_m denote the transverse membrane resistance and capacitance respectively. c_i denotes the (usually negligible) axial capacitance (shown using dotted lines) which ensures that the thermal noise has a bounded variance.

In the limit of large f, $S_{Vth}(f) \sim f^{-1/2}$, the indefinite integral of which diverges. This divergence is not due to r_m, but due to r_i. The noise due to r_m alone is of finite variance since the cable introduces a finite bandwidth. The resolution of this non-physical phenomenon lies in realizing that a pure resistance is a non-physical idealization. The cytoplasm is associated with a longitudinal capacitance in addition to its axial resistance, since current flow through the cytoplasm does not occur instantaneously. Ionic mobility is much smaller than that of electrons and charge accumulation takes place along the cytoplasm as a consequence. This can be modeled by the addition of an effective capacitance, c_i (in dotted lines in Figure 2) in parallel with r_i. Now, $S_{Vth}(f)$ is given by

$$S_{Vth}(f) = \frac{2kT\sqrt{r_i r_m}}{[\,(1+\theta_1^2)\,(1+\theta_2^2)\,]^{1/4}}\ \cos\left(\frac{\tan^{-1}\theta_1 + \tan^{-1}\theta_2}{2}\right) \tag{13}$$

where

$$\theta_1 = 2\pi f \tau_m \qquad \text{and} \qquad \theta_2 = 2\pi f \tau_i$$

where τ_i is the time constant of the axial RC segment. τ_i is usually very low, on the order of 3 μsec (Rosenfalck, 1969). In this case, for large f, $S_{Vth}(f) \sim f^{-2}$, thus its integral converges and σ^2_{Vth} remains finite.

The additional filtering due to the cytoplasmic capacitances imposes a finite bandwidth on the system, rendering the variance finite. Since $\tau_i \ll \tau_m$, its effect is significant only at very large frequencies, as is shown in Figure 3. Thus, neglecting the noise due to the cytoplasmic resistance is a very reasonable approximation for our frequency range of interest (1–1000 Hz).

2.2 Channel Noise

The membrane conductances we consider here are a consequence of microscopic, stochastic ionic channels (Hille, 1992). Since these channels open and close randomly, fluctuations in the number of channels constitutes a significant source of noise. In this section, we restrict the discussion to voltage-gated channels. However, ligand-gated channels can also be analyzed using the techniques discussed here. In a detailed Appendix, available over the Web[3], we present an analysis of the noise due to channel fluctuations for a simple two-state channel model for completeness. We apply well-known results from the theory of Markov processes, reviewed in DeFelice, (1981) and Johnston & Wu, (1995), to Hodgkin-Huxley-like models of voltage-gated K^+ and Na^+ channels. It is straightforward to extend these results to any other channel type with discrete states.

[3] `http:/www.klab.caltech.edu/~quixote/publications.html`

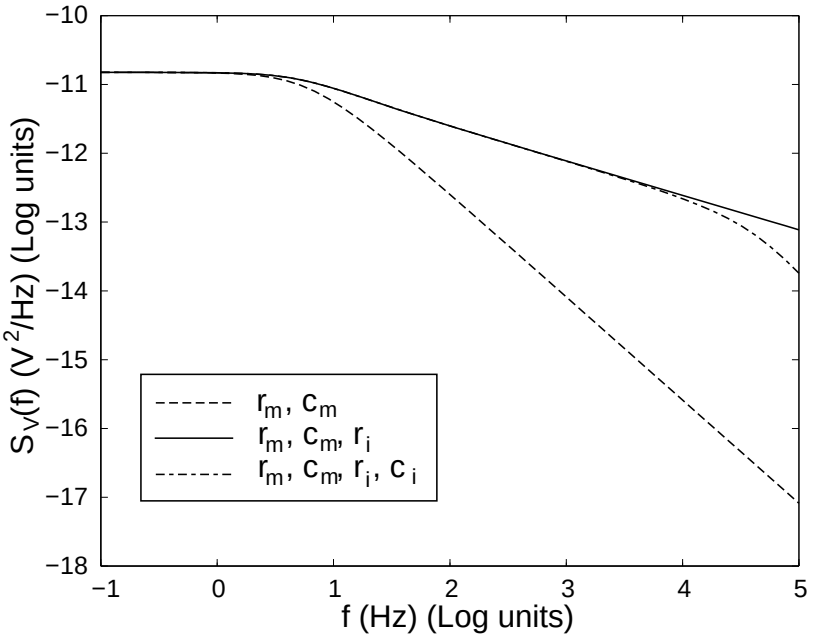

Figure 3: **Thermal Noise models for an Infinite 1-D Cable.** Comparison of power spectral densities of thermal voltage noise in an infinite cable corresponding to different assumptions. When the contribution due to the cytoplasmic resistance r_i is neglected (labeled as r_m, c_m), $S_{Vth}(f)$ represents the current noise due to the trans-membrane resistance r_m filtered by the Green's function of the infinite cable. $S_{Vth}(f) \sim f^{-3/2}$ for large f. When noise due to r_i is included (labeled as r_m, c_m, r_i) and eq. 12 is used, $S_{Vth}(f) \sim f^{-1/2}$ and the resulting variance is infinite. When filtering due to cytoplasmic capacitance c_i is taken into account (labeled as r_m, c_m, r_i, c_i) and eq. 13 is used, $S_{Vth}(f) \sim f^{-2}$. Since the integral of this power spectrum is bounded, the variance remains finite. Parameter values: $R_m = 40{,}000\ \Omega/\mathrm{cm}^2$, $R_i = 200\ \Omega\mathrm{cm}$, $\tau_m = 30$ msec, $\tau_i = 3\ \mu$sec.

2.2.1 K^+ channel noise

The seminal work by Hodgkin and Huxley (Hodgkin & Huxley, 1952) represents the first and very successful attempt at explaining the nature of membrane excitability in terms of voltage-gated particles. Most of our present understanding of membrane channels has been directly or indirectly influenced by their ideas (Hille, 1992).

In the Hodgkin-Huxley formulation, a K^+ channel comprises of four identical two-state subunits. The K^+ channel conducts only when all the sub-units are in their open states. Each sub-unit can be regarded as a two-state binary switch (like the model above) where the rate constants (α and β) depend on V_m. Hodgkin and Huxley used data from voltage-clamp experiments on the giant squid axon to obtain empirical expressions for this voltage dependence. Since the sub-units are identical, the channel can be in one of five states; from the state corresponding to all sub-units closed to the open state in which all sub-units are open. In general, a channel composed of n sub-units has $n+1$ distinct states if all the sub-units are identical and 2^n states if all the sub-units are distinct. The simplest kinetic scheme corresponding to a K^+ channel can be written as

$$\begin{array}{ccccccccc} C_0 & \underset{\beta_n}{\overset{4\alpha_n}{\rightleftharpoons}} & C_1 & \underset{2\beta_n}{\overset{3\alpha_n}{\rightleftharpoons}} & C_2 & \underset{3\beta_n}{\overset{2\alpha_n}{\rightleftharpoons}} & C_3 & \underset{4\beta_n}{\overset{\alpha_n}{\rightleftharpoons}} & O \\ (1) & & (2) & & (3) & & (4) & & (5) \end{array}$$

where C_i denotes the state in which i sub-units are open, O is the open state with all sub-units open. Thus, the evolution of a single K^+ channel can be a regarded as a five state Markov process with the following state

transition matrix:

$$\mathbf{Q}_K = \begin{bmatrix} -4\alpha_n & 4\alpha_n & 0 & 0 & 0 \\ \beta_n & -(3\alpha_n+\beta_n) & 3\alpha_n & 0 & 0 \\ 0 & 2\beta_n & -(2\alpha_n+2\beta_n) & 2\alpha_n & 0 \\ 0 & 0 & 3\beta_n & -(\alpha_n+3\beta_n) & \alpha_n \\ 0 & 0 & 0 & 4\beta_n & -4\beta_n \end{bmatrix} .$$

$\mathbf{Q}_K$ is a singular matrix with 4 non-zero eigenvalues which correspond to the cut-off frequencies in the K^+ current noise spectrum. If the probability of a sub-unit being open is denoted by $n(t)$, the open probability of a single K^+ channel, p_K is equal to $n(t)^4$. At steady state, the probability of a sub-unit being open at time t given that it was open at $t = 0$ ($\Pi_{55}(t)$ according to our convention) is given by

$$\Pi_{55}(t) = n_\infty + (1 - n_\infty)e^{-|\tau|/\theta_n} , \tag{14}$$

where

$$n_\infty = \frac{\alpha_n}{\alpha_n + \beta_n} \text{ and } \theta_n = \frac{1}{\alpha_n + \beta_n} \tag{15}$$

denote the steady-state open probability and relaxation time constant of the n sub-unit respectively. Thus, the auto-covariance of the current fluctuations due to the random opening and closing of K^+ channels in the nerve membrane can be written by analogy,

$$\begin{aligned} C_{IK}(\tau) &= \eta_K \gamma_K^2 (V_m - E_K)^2 \left[\Pi_{55}(\tau)^4 n_\infty^4 - n_\infty^8\right] & (16) \\ &= \eta_K \gamma_K^2 (V_m - E_K)^2 \left[n_\infty^4 \{n_\infty + (1 - n_\infty)e^{-|\tau|/\theta_n}\}^4 - n_\infty^8\right] , & (17) \end{aligned}$$

where η_K, γ_K and E_K denote the K^+ channel density in the membrane, the open conductance of a single K^+ channel and the potassium reversal potential respectively. On expansion we obtain,

$$C_{IK}(\tau) = \eta_K \gamma_K^2 (V_m - E_K)^2 n_\infty^4 \sum_{i=1}^{4} \binom{4}{i} (1 - n_\infty)^i n_\infty^{4-i} e^{-i|\tau|/\ \theta_n} \tag{18}$$

$$\text{where } \binom{n}{i} = \frac{n!}{(n-i)!\ i!} .$$

The variance of the K^+ current, $\sigma_K^2 = C_{IK}(0)$, is

$$\begin{aligned} \sigma_{IK}^2 &= \eta_K \gamma_K^2 (V_m - E_K)^2 n_\infty^4 (1 - n_\infty^4) & (19) \\ &= \eta_K \gamma_K^2 (V_m - E_K)^2 p_K (1 - p_K) . & (20) \end{aligned}$$

Taking the Fourier transform of $C_{IK}(\tau)$ gives us the power spectrum of the K^+ current noise

$$S_{IK}(f) = \eta_K \gamma_K^2 (V_m - E_K)^2 n_\infty^4 \sum_{i=1}^{4} \binom{4}{i} (1 - n_\infty)^i n_\infty^{4-i} \frac{2\ \theta_n/i}{1 + 4\pi^2 f^2 (\theta_n/i)^2} . \tag{21}$$

Notice that $S_{IK}(f)$ is given by a sum of 4 Lorentzian functions with different amplitude and cut-off frequencies. For $n_\infty \ll 1$, one can obtain a useful approximation for $S_{IK}(f)$

$$\begin{aligned} S_{IK}(f) &\approx \eta_K \gamma_K^2 (V_m - E_K)^2 n_\infty^4 (1 - n_\infty)^4 \frac{2\ \theta_n/4}{1 + 4\pi^2 f^2 (\theta_n/4)^2} & (22) \\ &\approx \frac{S_{IK}(0)}{1 + (f/f_K)^2} \quad (\text{units of } A^2/\text{Hz}) , & (23) \end{aligned}$$

where

$$S_{IK}(0) = \frac{\eta_K}{2}\gamma_K^2 (V_m - E_K)^2 n_\infty^4 (1-n_\infty)^4 \theta_n \quad \text{and} \quad f_K = \frac{4}{2\pi\theta_n}\,. \tag{24}$$

For small values of n_∞, the transitions $O \rightarrow C_3$ and $C_0 \rightarrow C_1$ dominate and the power spectrum can be approximated by a single Lorentzian with amplitude $S_{IK}(0)$ and cut-off frequency f_K. In this case the bandwidth[4] of K^+ current noise is given by $B_K \approx 1/\theta_n$. This approximation holds when the membrane voltage V_m is close to its resting potential V_{rest}.

2.2.2 Na^+ channel noise

The Hodgkin-Huxley Na^+ current is characterized by three identical activation subunits denoted by m and an inactivation sub-unit denoted by h. The Na^+ channel conducts only when all the m sub-units are open and the h sub-unit is not inactivated. Each of the sub-units may flip between their open (respectively, not inactivated) and closed (respectively, inactivated) states with the voltage-dependent rate constants α_m and β_m (respectively, α_h and β_h) for the m (respectively, h) sub-unit. Thus, the Na^+ channel can be in one of eight states from the state corresponding to all m sub-units closed and the h sub-unit inactivated to the open state with all m sub-units open and the h sub-unit not inactivated:

$$\begin{array}{ccccccc}
(1) & & (2) & & (3) & & (4) \\
C_0 & \underset{\beta_m}{\overset{3\alpha_m}{\rightleftharpoons}} & C_1 & \underset{2\beta_m}{\overset{2\alpha_m}{\rightleftharpoons}} & C_2 & \underset{3\beta_m}{\overset{\alpha_m}{\rightleftharpoons}} & O \\
\alpha_h \uparrow\downarrow \beta_h & & \alpha_h \uparrow\downarrow \beta_h & & \alpha_h \uparrow\downarrow \beta_h & & \alpha_h \uparrow\downarrow \beta_h \\
I_0 & \underset{\beta_m}{\overset{3\alpha_m}{\rightleftharpoons}} & I_1 & \underset{2\beta_m}{\overset{2\alpha_m}{\rightleftharpoons}} & I_2 & \underset{3\beta_m}{\overset{\alpha_m}{\rightleftharpoons}} & I_3 \\
(5) & & (6) & & (7) & & (8)
\end{array}$$

where C_i (respectively, I_i) denotes the state corresponding to i open sub-units of the m type and the h sub-unit not inactivated (respectively inactivated). The state transition matrix is given by

$$\mathbf{Q}_{Na} = \begin{bmatrix}
-(3\alpha_m+\beta_h) & 3\alpha_m & 0 & 0 & \beta_h & 0 & 0 & 0 \\
\beta_m & -(2\alpha_m+\beta_m+\beta_h) & 2\alpha_m & 0 & 0 & \beta_h & 0 & 0 \\
0 & 2\beta_m & -(2\beta_m+\alpha_m+\beta_h) & \alpha_m & 0 & 0 & \beta_h & 0 \\
0 & 0 & 3\beta_m & -(3\beta_m+\beta_h) & 0 & 0 & 0 & \beta_h \\
\alpha_h & 0 & 0 & 0 & -(3\alpha_m+\alpha_h) & 3\alpha_m & 0 & 0 \\
0 & \alpha_h & 0 & 0 & \beta_m & -(2\alpha_m+\beta_m+\alpha_h) & 2\alpha_m & 0 \\
0 & 0 & \alpha_h & 0 & 0 & 2\beta_m & -(\alpha_m+2\beta_m+\alpha_h) & \alpha_m \\
0 & 0 & 0 & \alpha_h & 0 & 0 & 3\beta_m & -(3\beta_m+\alpha_h)
\end{bmatrix}$$

Q_{Na} has 7 non-zero eigenvalues and so the Na^+ channel has 7 time constants. Thus, the Na^+ current noise spectrum can be expressed as a sum of 7 Lorentzians with cut-off frequencies corresponding to these time constants. The auto-covariance of the current fluctuations due to the sodium channels is given as

$$\begin{aligned}
C_{INa}(\tau) \quad = \quad & \eta_{Na}\gamma_{Na}^2 (V_m - E_{Na})^2 \Big[m_\infty^3 h_\infty \{m_\infty + (1-m_\infty)e^{-|\tau|/\theta_m}\}^3 \\
& \{h_\infty + (1-h_\infty)e^{-|\tau|/\theta_h}\} - m_\infty^6 h_\infty^2 \Big]\,,
\end{aligned} \tag{25}$$

[4] Defined as $B_K = \sigma_{IK}^2 / 2\, S_{IK}(0)$, the variance divided by the twice the magnitude of the power spectrum.

where η_{Na}, γ_{Na} and E_{Na} denote the Na^+ channel density, the Na^+ single channel conductance and the sodium reversal potential respectively.

$$m_\infty = \frac{\alpha_m}{\alpha_m + \beta_m} \quad \theta_m = \frac{1}{\alpha_m + \beta_m} \tag{26}$$

$$h_\infty = \frac{\alpha_h}{\alpha_h + \beta_h} \quad \theta_h = \frac{1}{\alpha_h + \beta_h} \tag{27}$$

denote the corresponding steady-state values and time constants of the m and h sub-units. The variance can be written as

$$\sigma^2_{INa} = \eta_{Na}\gamma^2_{Na}(V_m - E_{Na})^2 m^3_\infty h_\infty (1 - m^3_\infty h_\infty) \tag{28}$$

$$= \eta_{Na}\gamma^2_{Na}(V_m - E_{Na})^2 p_{Na}(1 - p_{Na})\,, \tag{29}$$

where $p_{Na} = m^3_\infty h_\infty$ is the steady-state open probability of a Na^+ channel. The power spectrum, obtained by taking the Fourier transform of $C_{INa}(\tau)$, is given by a combination of 7 Lorentzian components. The general expression is tedious and lengthy to express and so we shall restrict ourselves to a reasonable approximation. For $m_\infty \ll 1$ and $h_\infty \approx 1$, around the resting potential.

$$qS_{INa}(f) \approx \eta_{Na}\gamma^2_{Na}(V_m - E_{Na})^2 m^3_\infty (1 - m_\infty)^3 h^2_\infty \frac{2\ \theta_m/3}{1 + 4\pi^2 f^2 (\theta_m/3)^2} \tag{30}$$

$$\approx \frac{S_{INa}(0)}{1 + (f/f_{Na})^2} \quad (\text{units of } \mathrm{A}^2/\mathrm{Hz})\,, \tag{31}$$

where

$$S_{INa}(0) = \frac{2\eta_{Na}}{3}\gamma^2_{Na}(V_m - E_{Na})^2 m^3_\infty h_\infty (1 - m_\infty)^3 h_\infty \theta_m \ \text{ and } \ f_{Na} = \frac{3}{2\pi\theta_m}\,. \tag{32}$$

Thus, for voltages close to the resting potential, $S_{INa}(f)$ can be approximated by a single Lorentzian. The bandwidth of Na^+ current noise under this approximation is given by $B_{Na} \approx 3/(4\,\theta_m)$.

In general, the magnitude and shape of the power spectrum is determined by the kinetics of corresponding single channels. For, any given state transition matrix describing the channel kinetics, we can derive expressions for the noise power spectral densities using the procedure outlined above. For most kinetic models, when $V_m \approx V_{rest}$, the single Lorentzian approximation suffices. A variety of kinetic schemes modeling different types of voltage-gated ion channels exist in the literature. We shall choose a particular scheme to work with but the formalism is very general and can be used to study arbitrary finite-state channels.

2.3 Synaptic Noise

In addition to voltage-gated channels which open and close in response to membrane potential changes, dendrites (and the associated spines, if any) are also awash in ligand-gated synaptic receptors. We shall restrict our attention to the family of channels specialized for mediating fast chemical synaptic transmission in a voltage-independent manner, excluding for now NMDA-type of currents.

Chemical synaptic transmission is usually understood as a conductance change in the post-synaptic membrane caused by the release of neurotransmitter molecules from the presynaptic neuron in response to presynaptic membrane depolarization. A commonly used function to represent the time course of the postsynaptic change in response to a presynaptic spike is the *alpha* function (Rall, 1967; Koch, 1999)

$$g_\alpha(t) = \frac{g_{peak}\, e}{t_{peak}}\ t\, e^{-t/t_{peak}}\ u(t)\,, \tag{33}$$

where g_{peak} denotes the peak conductance change and t_{peak} is the time-to-peak of the conductance change. $u(t)$ is the unit step function which ensures that $g_\alpha(t) = 0$ for $t < 0$. More general kinetic descriptions have been proposed (Destexhe *et al.*, 1994), but are not considered here.

We shall assume that for a spike train $s(t) = \sum_j \delta(t - t_j)$, modeled as a sum of impulses occurring at times t_j, the postsynaptic change is given by a sum of time-shifted conductance functions,

$$g_{Syn}(t) = \sum_j g_\alpha(t - t_j)\,. \tag{34}$$

This means that each spike causes the same conductance change and that the conductance change due to a sequence of spikes is the sum of the changes due to individual spikes in the train. For now, we ignore the effect of paired-pulse facilitation or depression (Abbott *et al.*, 1997; Tsodyks & Markram, 1997). The synaptic current $i_{Syn}(t)$ is given by

$$i_{Syn}(t) = g_{Syn}(t)\,(V_m - E_{Syn})\,, \tag{35}$$

where E_{Syn} is the synaptic reversal potential. As before, we assume that the synaptic current is small enough so that V_m is nearly constant. If the spike train of the presynaptic neuron can be modeled as a homogeneous Poisson process with mean firing rate λ_n, one can compute the mean and variance of the synaptic current arriving at the membrane using Campbell's theorem (Papoulis, 1991):

$$\langle i_{Syn}(t)\rangle = \lambda_n (V_m - E_{Syn}) \int_0^\infty g_\alpha(t)\; dt\,, \tag{36}$$

$$\sigma^2_{ISyn} = \lambda_n (V_m - E_{Syn})^2 \int_0^\infty (g_\alpha(t))^2\; dt\,. \tag{37}$$

It is straightforward to compute the auto-covariance $C_{ISyn}(\tau)$ of the synaptic current,

$$C_{ISyn}(\tau) = \lambda_n (V_m - E_{Syn})^2\, g_\alpha(\tau) * g_\alpha(-\tau)\,, \tag{38}$$

$$= \lambda_n (V_m - E_{Syn})^2 \int_0^\infty g_\alpha(t)\; g_\alpha(t+\tau)\; dt\,. \tag{39}$$

Similarly, the power spectral density of the synaptic current is given by

$$S_{ISyn}(f) = \mathcal{F}\{C_{ISyn}(\tau)\} = \lambda_n\,(V_m - E_{Syn})^2 \mid G_\alpha(f)\mid^2\,, \tag{40}$$

where

$$G_\alpha(f) = \mathcal{F}\{g_\alpha(t)\} = \int_0^\infty g_\alpha(t)\; e^{-j2\pi f t}\; dt \tag{41}$$

denotes the Fourier transform of $g_\alpha(t)$. For the alpha function,

$$G_\alpha(f) = \frac{e\; g_{peak}\; t_{peak}}{(1 + j\,2\pi f t_{peak})^2}\,. \tag{42}$$

It has been shown that if the density of synaptic innervation is high or alternatively if the firing rates of the presynaptic neurons are high and the conductance change due to a single impulse is small, the synaptic current tends to a Gaussian process (Tuckwell & Wan, 1980). This is called the *diffusion approximation*. Since a Gaussian process is completely specified by its power spectral density, one only needs to compute the power spectrum of

current noise due to random synaptic activity. If η_{Syn} denotes the synaptic density, the variance, auto-covariance and the power spectral density of the synaptic current noise are given by

$$\sigma^2_{ISyn} = \eta_{Syn}\ \lambda_n \left(\frac{g_{peak}\ e}{2}\right)^2 (V_m - E_{Syn})^2\, t_{peak}\,, \tag{43}$$

$$C_{ISyn}(\tau) = \sigma^2_{ISyn}\ [1 + |\tau|\tau_{peak}]\ e^{-|\tau|/t_{peak}}\,, \tag{44}$$

$$S_{ISyn}(f) = \eta_{Syn}\ \lambda_n\ \frac{[e\ g_{peak}\ t_{peak}\ (V_m - E_{Syn})]^2}{[1 + (2\pi f t_s)^2]}\,, \tag{45}$$

$$= \frac{S_{ISyn}(0)}{[1 + (f/f_{Syn})^2]^2} \quad (\text{units of } \mathrm{A}^2/\mathrm{Hz})\,, \tag{46}$$

where

$$S_{ISyn}(0) = 4\ \sigma^2_{ISyn}\ t_{peak} \quad \text{and} \quad f_{Syn} = \frac{1}{2\pi\, t_{peak}}\,. \tag{47}$$

A power spectrum of the above form is called a *double Lorentzian* spectrum. As before, the power spectrum can be represented in terms of its DC amplitude $S_{Syn}(0)$, and its cut-off frequency f_{Syn}. The double Lorentzian spectrum falls twice as fast with the logarithm of frequency as compared to a single Lorentzian because of the double pole at f_{Syn}. Thus, f_{Syn} is the frequency for which the magnitude of the power spectrum is one fourth of its amplitude. Using our definition of bandwidth, the bandwidth of the synaptic current noise, $B_{Syn} = \frac{\pi}{4} f_{Syn} = 1/8\ t_{peak}$.

2.4 Other Sources of Noise

In addition to these sources, there are several other sources of noise in biological membranes (Verveen & DeFelice, 1974; Neher & Stevens, 1977; DeFelice, 1981). The neuronal membrane contains ionic channels (Hille, 1992) with different kinetics, in different proportions. Random fluctuations in the number of these channels also contributes to membrane noise. Additionally, myriad types of ligand-gated channels also contribute to the noise level. Using the analysis above, it is clear that if accurate estimates of their relevant parameters (densities, kinetics and so on) are made available, one can potentially compute their contributions to membrane noise as well.

Other types of membrane noise are $1/f$ noise (Neumcke, 1978; Clay & Shlesinger, 1977), (also called *excess* or *flicker noise*), shot noise due to ions in transit through leak channels or pores (Frehland & Faulhaber, 1980; Frehland, 1982), carrier-mediated transport noise in ionic pumps and burst noise. We did not include these in our analysis, either due to a lack of a sound theoretical understanding of their origin or the relative insignificance of their magnitudes.

A summary of the expressions we have used to characterize the noise sources is provided in Table 1. We have modeled the sources as current fluctuations by assuming that the membrane voltage was clamped at V_m. The magnitude and nature of the current fluctuations depend on the kinetics and the driving potential, and thus on V_m. In the next section, we investigate the effect of embedding a membrane patch with these noise sources. There we assume that the current fluctuations are small enough so that V_m does not deviate significantly from its resting value, V_{rest}. In general, this approximation must be verified for the different noise sources considered. We use the expressions in Table 1 to identify the contribution of each noise source to the total membrane voltage noise for different biophysically relevant parameter values. In the following paper, deriving similar expressions for membrane noise sources in a linear cable, we quantify the information lost by synaptic signal as it propagates down a dendrite due to these noise sources.

Noise type	K^+	Na^+	Synaptic
σ_I^2	$\eta_K\ I_{K,max}^2\ p_K\,(1-p_K)$	$\eta_{Na}\ I_{Na,max}^2\ p_{Na}(1-p_{Na})$	$(e/2)^2\ \eta_{Syn}\ \lambda_n\ I_{Syn,max}^2 t_{peak}$
$C_I(\tau)/\sigma_I^2$	$\exp(-\lvert\tau\rvert/4\ \theta_n)$	$\exp(-\lvert\tau\rvert/3\ \theta_m)$	$(1+\lvert\tau\rvert/t_{peak})\ \exp(-\lvert\tau\rvert/t_{peak})$
f_c	$4/(2\pi\theta_n)$	$3/(2\pi\theta_m)$	$1/(2\pi t_{peak})$
$S_I(0)$	$\sigma_{IK}^2\ \theta_n/2$	$2\ \sigma_{INa}^2\ \theta_m/3$	$4\ \sigma_{ISyn}^2\ t_{peak}$
$S_I(f)/S_I(0)$	$1/[1+(f/f_K)^2]$	$1/[1+(f/f_{Na})^2]$	$1/[1+(f/f_{Syn})^2]^2$
B	$1/\theta_n$	$3/(4\,\theta_m)$	$1/(8\,t_{peak})$

Table 1: Summary of expressions used to characterize current noise due to conductance fluctuations (K^+, Na^+) and random synaptic activity. For Na^+ and K^+ we have made the assumption that the membrane voltage is around the resting value. $I_{K,max} = \gamma_K(V_m - E_K)$, $I_{Na,max} = \gamma_{Na}(V_m - E_{Na})$ and $I_{Syn,max} = g_{peak}(V_m - E_{Syn})$ denote the maximum possible values of current through a single K^+ channel, Na^+ channel and synapse respectively. Since densities are expressed in terms of per unit area, σ_I^2, and S_I have units of $A^2/\mu m^2$ and $A^2/Hz\ \mu m^2$ respectively.

3 Noise in a Membrane Patch

Consider a patch of neuronal membrane of area A, containing Hodgkin-Huxley type rapid sodium I_{Na} and delayed rectifier I_K currents as well as fast (AMPA) voltage-independent synapses. If the patch is small enough, it can be considered as a single point, making the membrane voltage solely a function of time. We shall make this "point-like" assumption here and defer analysis of the general case of spatial dependence of the potential to the following paper.

Let C denote the capacitance of the patch, given by the product $C = C_m A$. The passive membrane conductance due to voltage-independent leak channels is given by g_L. Current injected into the membrane from all other sources is denoted by $I_{inj}(t)$. Since the area of the patch is known, the absolute values of the conductances can be obtained by multiplying their corresponding specific values by the patch area A. On the other hand, if we wish to continue working with specific conductances and capacitances, the injected current needs to be divided by A to obtain the current density. Here we use the former convention. The electric circuit corresponding to the membrane patch is shown in Figure 4. Using Kirchoff's law we have,

$$C\frac{\mathrm{d}V_m}{\mathrm{d}t} + g_K(V_m - E_K) + g_{Na}(V_m - E_{Na}) + g_{Syn}(V_m - E_{Syn}) + g_L(V_m - E_L) = I_{inj}\,. \tag{48}$$

Since the ion channels and synapses are stochastic, g_K, g_{Na} and g_{Syn} in the above equation are stochastic processes. Consequently, eq. 48 is, in effect, a *stochastic differential equation*. Moreover, since the active conductances (g_K and g_Na) depend on V_m, eq. 48 is non-linear in V_m and in all likelihood intractable to theoretical analysis. However, as a consequence of the assumption that the system is in quasi-equilibrium, one can effectively linearize the active conductances and express them as deviations around their respective steady-state equilibrium values,

$$g_K = g_K^o + \tilde{g}_K, \tag{49}$$
$$g_{Na} = g_{Na}^o + \tilde{g}_{Na}, \tag{50}$$
$$g_{Syn} = g_{Syn}^o + \tilde{g}_{Syn}, \tag{51}$$
$$V_m = V^o + V\,. \tag{52}$$

This perturbative approximation can easily be verified by self-consistency. If the approximation is valid, the deviations (V) of the membrane voltage from the resting voltage should be small. For the cases we consider, the membrane fluctuations are indeed small and so the approximation holds. However, in general, the validity of this approximation needs to be verified on a case by case basis.

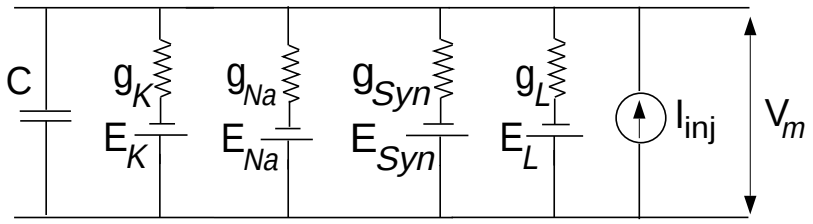

Figure 4: **Equivalent Electric Circuit of a Membrane Patch.** C denotes the patch capacitance and, g_L, the passive membrane resistance due to leak channels. The membrane also contains active channels (K^+, Na^+) and fast voltage-independent synapses, their conductances are represented by g_K, g_{Na} and g_{Syn} respectively. Current injected from other sources is denoted by I_{inj}.

V^o is chosen such that it satisfies the equation

$$V^o = \frac{g_K^o\, E_K + g_{Na}^o\, E_{Na} + g_{Syn}^o\, E_{Syn} + g_L\, E_L}{G} \tag{53}$$

where $G = g_K^o + g_{Na}^o + g_{Syn}^o + g_L$ is the total baseline input conductance of the patch, equal to the sum of all the baseline conductances. Similarly, $\tilde{g} = \tilde{g}_K + \tilde{g}_{Na} + \tilde{g}_{Syn}$ denotes the total random component of the patch conductance. Substituting for eqs. 49-52 in eq. 48 gives us the following equation,

$$C\frac{\mathrm{d}V_m}{\mathrm{d}t} + G(V_m - V^o) + \tilde{g}_K(V_m - E_K) + \tilde{g}_{Na}(V_m - E_{Na}) + \tilde{g}_{Syn}(V_m - E_{Syn}) = I_{inj}\,. \tag{54}$$

Since the steady-state (resting) solution of eq. 48 is $V_m = V_{rest}$, we can choose to linearize about the resting potential, $V^o = V_{rest}$. The effective time constant of the patch depends on G and is given by $\tau = C/G$. When $V_m(t) \approx V_{rest}$, g_L is usually the dominant conductance and so $G \approx g_L$. However, during periods of intense synaptic activity, or for strongly excitable systems, G can be significantly larger than g_L (Bernander *et al.*, 1991; Rapp *et al.*, 1992). If no external current is injected, the only other source of current is the thermal current noise and I_{inj} is equal to I_{th}.

Expressing $V_m(t)$ as deviations around V_{rest} in the form of the variable $V(t) = V_m(t) - V_{rest}$ allows us to simplify eq. 54 to

$$\tau\frac{\mathrm{d}V}{\mathrm{d}t} + (1+\delta)\,V = \frac{I_n}{G}\,, \tag{55}$$

where

$$\delta = \frac{\tilde{g}_K + \tilde{g}_{Na} + \tilde{g}_{Syn}}{G} = \frac{\tilde{g}}{G}\,, \tag{56}$$

$$I_n = \tilde{g}_K(E_K - V_{rest}) + \tilde{g}_{Na}(E_{Na} - V_{rest}) + \tilde{g}_{Syn}(E_{Syn} - V_{rest}) + I_{th}\,. \tag{57}$$

The circuit diagram corresponding to the above is shown in Figure 5. The random variable δ corresponds to fluctuations in the membrane conductance due to synaptic and channel contributions and has a multiplicative effect on V. On the other hand, I_n corresponds to an additive current noise source arising due conductance fluctuations at V_{rest} ($V = 0$). We assume that the conductance fluctuations about the V_{rest} are zero-mean wide-sense-stationary (WSS) processes. Since the noise sources have different origins, it is also plausible to assume that they are statistically independent. Thus, I_n is also a zero-mean WSS random process, $\langle I_n \rangle = 0$.

Our perturbative approximation implies that the statistical properties of the processes δ and I_n are evaluated at $V = 0$. We are unable to solve eq. 55 analytically because of the nonlinear (multiplicative) relationship between δ and V. However, since the membrane voltage does not change significantly, in most cases, the deviations of

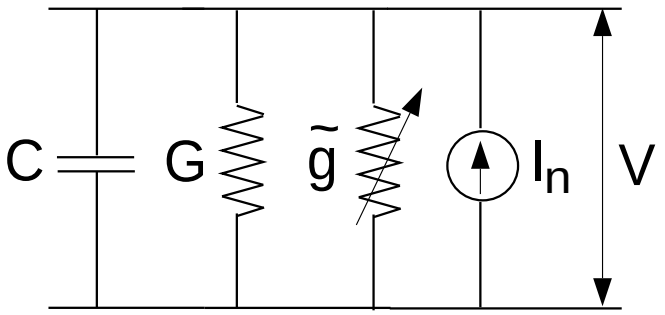

Figure 5: **Equivalent Electric Circuit After Linearization.** Circuit diagram of the membrane patch containing different noise sources, close to equilibrium. The membrane voltage V is measured as a deviation from the resting value V_{rest}. G is the deterministic resting conductance of the patch and $\tilde{g}$ is the random component due to the fluctuating conductances. The conductance fluctuations also give rise to an additive current noise source I_n.

the conductances are small compared to the resting conductance of the cell[5], implying $\delta \ll 1$, which allows us to further simplify eq. 55 to

$$\tau \frac{\mathrm{d}V}{\mathrm{d}t} + V = \frac{I_n}{G}\,. \tag{58}$$

This equation corresponds to a linear system driven by an additive noise source. It is straight-forward to derive the statistical properties of V in terms of the statistical properties of I_n. For instance, the power spectral density of $V(t)$, $S_V(f)$ can be written in terms of power spectral density of I_n, $S_{In}(f)$ as,

$$S_V(f) = \frac{S_{In}(f)}{G^2\left[1 + (2\pi f \tau)^2\right]}\,. \tag{59}$$

Since the noise sources are independent,

$$S_{In}(f) = A\left[S_{IK}(f) + S_{INa}(f) + S_{ISyn}(f) + S_{Ith}(f)\right]. \tag{60}$$

Using the single Lorentzian approximations for the K^+ and Na^+ spectra, one can write an expression for the variance of the voltage noise as,

$$\begin{aligned}\sigma_V^2 \;\approx\; & \frac{\pi A}{G^2}\left[S_{IK}(0)\frac{f_m f_K}{f_m + f_K} + S_{INa}(0)\frac{f_m f_{Na}}{f_m + f_{Na}} + \right. \\ & \left. S_{ISyn}(0)\frac{f_m f_{Syn}}{f_m + f_{Syn}}\frac{f_m^2 + f_{Syn} f_m - 2f_{Syn}^2}{f_m^2 - f_{Syn}^2} + S_{Ith}(0)\, f_m\right], \end{aligned} \tag{61}$$

where $f_m = 1/2\pi\tau$ is the cut-off frequency corresponding to the membrane's passive time constant.

3.1 Parameter Values

We consider a space-clamped cell body of a typical neocortical pyramidal cell as the substrate for our noisy membrane-patch model. Estimates of the somatic/dendritic Na^+ conductance densities in neocortical pyramidal cells range from 4 to 12 mS/cm^2 (Huguenard *et al.*, 1989; Stuart & Sakmann, 1994). We assume $\eta_{Na} = 2$ channels/μm^2 with $\gamma_{Na} = 20$ pS. K^+ channel densities are not known as reliably mainly because there are a multitude of different K^+ channel types. However, some recent experimental and computational studies (Hoffman *et al.*, 1997; Mainen & Sejnowski, 1998; Magee *et al.*, 1998; Hoffman & Johnston, 1998) provide estimates for

[5]The validity of this assumption can easily, and must, be verified on a case by case basis.

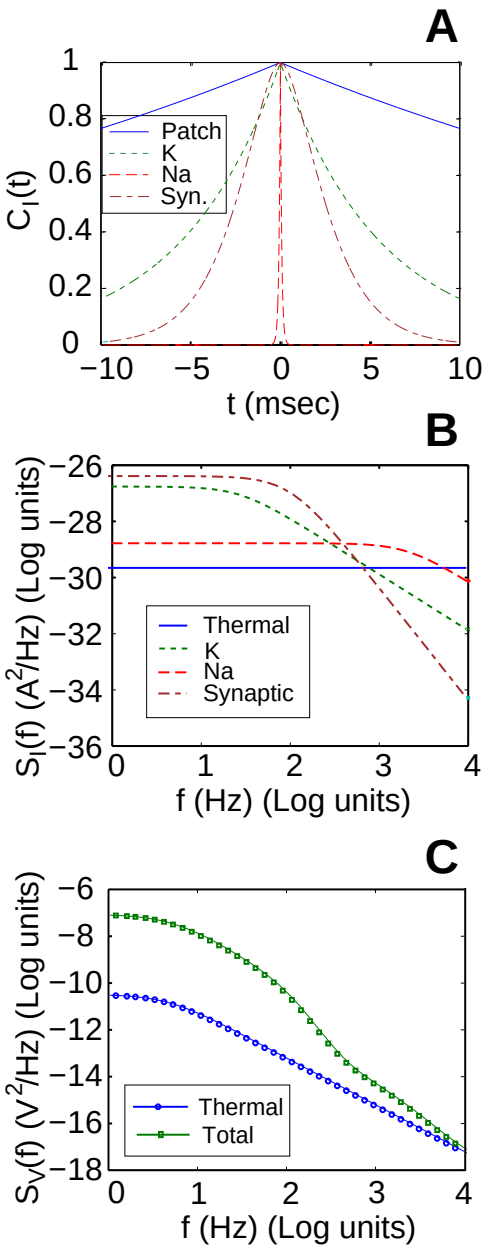

Figure 6: **Noise in a Somatic Membrane Patch.** **(A)** Comparison of the normalized correlation functions $C_I(t)/C_I(0)$ of the different noise sources with the autocorrelation of the Green's function of an RC circuit ($e^{-t/\tau}$), for parameter values summarized below. **(B)** Comparison of current power spectra $S_I(f)$ of the different membrane noise sources, *viz.*, thermal noise, K^+ channel noise, Na^+ channel noise and synaptic background noise as a function of frequency (upto 10 kHz). **(C)** Voltage spectrum $S_V(f)$ of the noise in a somatic patch due the influence of the above sources. Power spectrum of the voltage fluctuations due to thermal noise alone $S_{Vth}(f)$ is also shown for comparison. Summary of the parameters adopted from Mainen & Sejnowski (1998): R_m = 40 kΩ cm^2, C_m = 1 μF/cm^2, η_K = 1.5 channels per μm^2, η_{Na} = 2 channels per μm^2, η_{Syn} = 0.01 synapses per μm^2 with spontaneous firing rate λ_n = 0.5 Hz. E_K = -95 mV, E_{Na} = 50 mV, E_{Syn} = 0 mV, E_L = -70 mV, $\gamma_K = \gamma_{Na}$ = 20 pS. Synaptic parameters: g_{peak} = 100 pS, t_{peak} = 1.5 msec.

the K^+ densities in the soma and dendrites of cortical neurons. We choose η_K = 1.5 channels/μm^2, adopted from Mainen & Sejnowski, (1998). The channel kinetics and the voltage dependence of the rate constants also

Noise type	$A * S_I(0)$ (A^2/Hz)	$S_V(0)$ (V^2/Hz)	σ_V (mV)
Thermal	2.21×10^{-30}	3.14×10^{-11}	2.05×10^{-2}
K^+	1.74×10^{-27}	2.46×10^{-8}	5.33×10^{-1}
Na^+	1.67×10^{-28}	2.36×10^{-10}	5.59×10^{-2}
Synaptic	4.12×10^{-27}	5.84×10^{-8}	8.54×10^{-1}
Total	5.88×10^{-27}	8.33×10^{-8}	1.01

Table 2: Comparison of the magnitudes of the current power spectral densities ($A * S_I(0)$, units of A^2/Hz), the voltage power spectral densities ($S_V(0)$, units of V^2/Hz) and the voltage standard deviations (σ_V, units of mV) of the different noise sources (thermal, K^+, Na^+ conductance fluctuations and synaptic background) in a space-clamped somatic membrane patch.

correspond to Mainen *et. al.*, (1995). We use $R_m = 40{,}000\ \Omega\text{cm}^2$ and $C_m = 1\ \mu\text{F/cm}^2$ obtained from recent studies based on tight-seal whole cell recordings (Spruston *et al.*, 1994; Major *et al.*, 1994), giving a passive time constant of $\tau_m = 40$ msec. The entire soma is reduced to a single membrane patch of area $A = 1000\ \mu\text{m}^2$.

The number of synapses at the soma is usually small, which leads us to $\eta_{Syn} = 0.01$ synapses/μm^2, that is 10 synapses. Other synaptic parameters are: $g_{peak} = 100$ pS, $t_{peak} = 1.5$ msec, $\lambda_n = 0.5$ Hz. No account is made of synaptic transmission failure, but see Manwani & Koch, (1998) for an analysis of synaptic unreliability and variability.

4 Results

We compute the current and voltage power spectra (shown in Figure 6) over the frequency range relevant for fast computations for the biophysical scenario discussed above. Experimentally, the current noise spectrum can be obtained by performing a voltage-clamp experiment, while the voltage noise spectra can be measured under current-clamp conditions. The voltage noise spectrum includes the effect of filtering (which has a Lorentzian power spectrum) due to the passive RC circuit corresponding to the patch. In the companion manuscript (Manwani & Koch, 1999), we show that in a real neuron the cable properties of the system recorded from give rise to more complex behavior. Since we have modeled the membrane patch as a passive RC filter and regarded the active voltage-gated ion channels as pure conductances, we obtained monotonic low-pass voltage spectra. In general, as we have mentioned before, the small-signal membrane impedance due to voltage and time dependent conductances can exhibit resonance giving rise to band-pass characteristics in the voltage noise spectra (Koch, 1999).

The relative magnitudes of the current noise power spectral densities ($S_I(0)$) and the amplitudes of voltage noise due to each noise source (S_{Vi} and σ_{Vi}) are compared in Table 2.

The contribution of each noise source to the overall spectrum depends on the exact values of the parameters—including the channel kinetics—which can vary considerably across neuronal types and even from one neuronal location to another. For the parameter values we considered, thermal noise made the smallest contribution, and is at the limit of what is experimentally resolvable using modern amplifiers. Background synaptic noise due to spontaneous activity was the dominant component of neuronal noise. The magnitude of noise for the scenario we consider here is small enough to justify the perturbative approximation, but it can be expected that for small structures, especially thin dendrites or spines, the perturbative approximation might be violated. However, treating a dendritic segment as a membrane patch is not an accurate model for real dendrites where

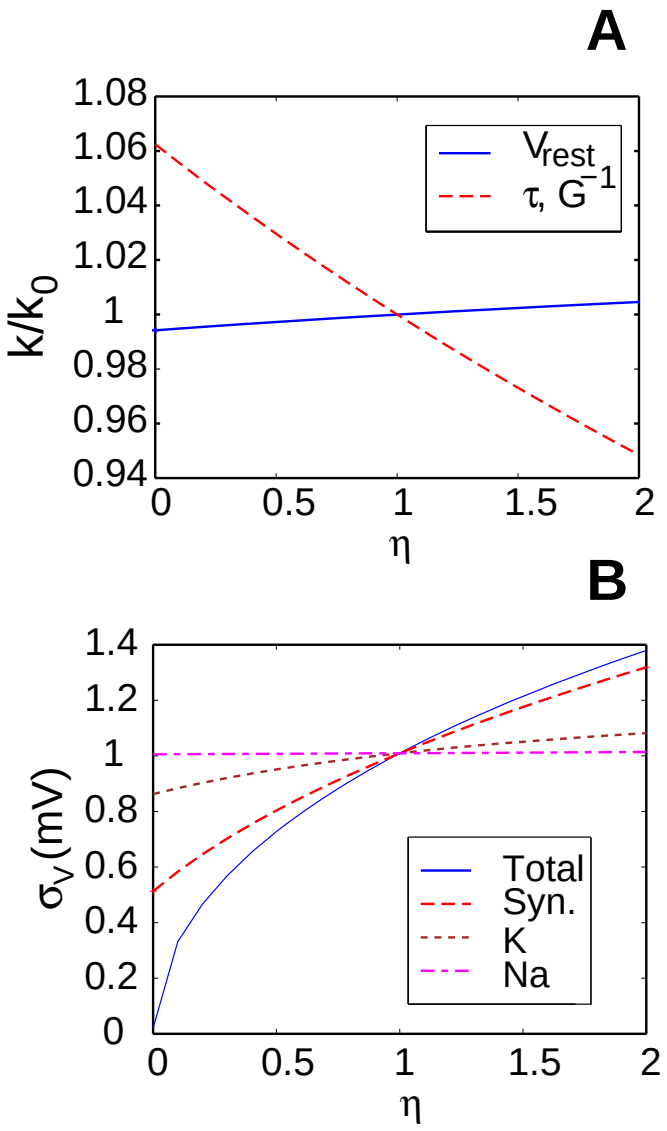

Figure 7: **Influence of Biophysical Parameters. (A)** Dependence of the passive membrane parameters (V_{rest}, τ) on the channel and synaptic densities. The K^+ and Na^+ channel densities and the synaptic density are scaled by the same factor η which varies from $\eta = 0$ (corresponding to a completely passive system) to $\eta = 2$. $\eta = 1$ corresponds to the nominal parameter values used to generate **Figure 6**. The membrane parameters (denoted generically by κ) are expressed as a ratio of their nominal values at $\eta = 1$ (denoted by κ_0). **(B)** Effect of varying individual densities (the remaining densities are maintained at their nominal values) on the magnitude of the voltage noise σ_V.

currents can flow longitudinally. We shall address this problem again in the context of noise in linear cables in the following paper.

There are numerous parameters in our analysis and it would be extremely tedious to consider the combinatorial effect of varying them all. We restrict ourselves to studying the effect of varying a few biological relevant parameters.

4.1 Dependence on Area

Notice that varying the patch area A does not affect the resting membrane potential V_{rest} or the passive membrane time constant τ. From eq. 59 one can deduce the scaling behavior of S_V with respect to A in a straightforward manner. The numerator increases linearly with A since the noise sources are independent and in parallel and so their contributions add. However, all the individual membrane conductances scale linearly with A, thus, the total conductance G also scales linearly with A. As a consequence, $S_V(f)$ and σ_V^2 scale inversely with A: the larger the area, the smaller the variance. Equivalently, σ_V scales inversely as the square root of A.

This might appear counterintuitive since the number of channels increases linearly with A, but can be understood as follows. The current fluctuations are integrated by the RC filter corresponding to the membrane patch and manifest as voltage fluctuations. As the area of the patch increases, the variance of the current fluctuations increases linearly but the input impedance decreases as well. Since the variance of the voltage fluctuations is proportional to the square of the impedance, the decrease in impedance more than offsets the linear increase due to the current and so the resulting voltage fluctuations are smaller. If all the channel and synaptic densities are increased by the same factor (a global increase in the number of channels), an identical scaling behavior is obtained.

This suggests that the voltage noise from small patches might be large. Indeed, it is plausible to assume that for small neurons, the voltage fluctuations can be large enough to cause "spontaneous" action potentials. This phenomenon of noise-induced oscillations has indeed be borne out by simulations (Skaugen & Wallœ, 1979; Skaugen, 1980; Strassberg & DeFelice, 1993; Schneidman *et al.*, 1998).

4.2 Dependence on Channel Densities

We first consider the effect of varying the different individual channel densities on the resting properties of the patch, that is on V_{rest}, G and τ. The K^+ and Na^+ channel densities and the synaptic densities (except g_L) are first scaled individually and then together by the same factor. We denote the scale parameter by η. When all densities are scaled together, $\eta = 0$ corresponds to a purely passive patch containing leak channels alone and $\eta = 1$ corresponds to the membrane patch scenario considered above (referred to as the nominal case). Similarly, when only the K^+ density is varied, $\eta = 0$ corresponds to a membrane patch without K^+ channels and $\eta = 1$ denotes the nominal value. The results of this exercise are summarized in Figure 7A. Instead of using absolute values for the quantities of interest, we normalize them with respect to their nominal values corresponding to $\eta = 1$. Notice that when all the densities, except leak, are varied from $\eta = 0$ to $\eta = 2$, V_{rest} varies (becomes more hyper-polarized) by less than 1% and τ and G^{-1} vary from about a 6% increase ($\eta = 0$) to a 5% decrease ($\eta = 2$). Despite the non-linearities due to the active K^+ and Na^+ conductances, it is noteworthy that the quantities vary almost linearly with η, further justifying our perturbative approximation.

The effect of varying individual densities on σ_V is explored in Figure 7B. In order to consider the contribution of a given process to the noise magnitude, we vary the associated density in a similar manner as above (η goes from 0 to 2), while maintaining the others at their nominal values. We also compare the individual profiles to the case when all densities are scaled by the same factor. It is clear from the figure that the synaptic noise is the dominant noise source. The noise magnitude drops approximately from 1 mV to 0.5 mV in the absence of synaptic input (as η varies goes from 1 to 0), but only to about 0.85 mV in the absence of K^+ channels. Varying the Na^+ density has a negligible effect on the noise magnitude. Similarly, the noise increases to 1.35 mV when the synaptic density is doubled ($\eta = 2$) with respect to its nominal values, but the increase to about 1.07 mV due to the doubling of K^+ density is much smaller.

5 Discussion

With this paper, we initiate a systematic investigation of how various neuronal noise sources influence and, ultimately, limit the ability of one-dimensional cable structures to propagate information. Ultimately, we are interested in answering such questions as, whether or not the length of the apical dendrite of a neocortical pyramidal cell is limited by considerations of signal-to-noise, what influences the noise level in the dendritic tree of some neuron endowed with voltage-dependent channels, how accurately can the time course of an synaptic signal be reconstructed from the voltage at the spike initiation zone, what is the channel capacity of an unreliable synapse onto a spine and so on. Our research program is driven by the hypothesis that noise fundamentally limits the precision, speed and accuracy of computation in the nervous system (Koch, 1999).

Providing satisfactory answers to these issues requires the characterization of the various neuronal noise sources that can cause loss of signal fidelity at different stages in the neuronal link. This is what we have undertaken in the present manuscript. The analysis of membrane noise has a long and successful history. Before the patch-clamp technique was developed, membrane noise analysis was traditionally used to provide indirect evidence for the existence of ionic channels and obtain estimates of their biophysical properties This has been admirably described in (DeFelice, 1981). Despite the universality of patch-clamp methods to study single channels today, noise analysis still remains a useful tool for certain problems (Traynelis & Jaramillo, 1998).

In the approaches mentioned above, noise analysis has been exploited as an investigative measurement technique. Our interest lies in understanding how the inherent sources of noise at the single-neuron level have bearing on the temporal precision with which neurons respond to sensory input or direct current injection. These questions have received renewed scrutiny in recent times. It is becomingly increasingly apparent how a transition from discrete, microscopic and stochastic channels is made to continuous, macroscopic and deterministic currents (Strassberg & DeFelice, 1993). Several attempts have also been made to explore if the rich dynamics of neuronal activity and the temporal reliability of neural spike trains can be explained in terms of microscopic fluctuations (Clay & DeFelice, 1983; DeFelice & Isaac, 1992; White *et al.*, 1995; Chow & White, 1996; Schneidman *et al.*, 1998). This paper reflects a continuation of this pursuit.

The key result of our approach is that we are able to derive closed-form expressions for the membrane voltage fluctuations due to the three dominant noise types in neuronal preparations: thermal, channel and synaptic noise. However, we obtain these results at a price. We assume that the deviations of the membrane potential about its resting value, as a result of "spontaneous" synaptic input and channels switching, are small. This allows us to make a perturbative approximation and express conductances changes as small deviations around their resting values, allowing us to treat them as sources of current noise. The validity of this supposition needs to be carefully evaluated empirically. This can be considered analogous to the linearization of non-linear differential equations about a quiescent point, the only difference being that the quantities being dealt with are stochastic. For a related approach, see Larsson *et. al.*, (1997).

This approximation enables us to write down a stochastic differential equation eq. 55 governing the dynamics of voltage fluctuations. Since we are unable to solve eq. 55 analytically, we invoke another simplifying assumption, namely that the conductance fluctuations are small compared to the total resting conductance. The validity of this assumption can also be easily verified. This assumption simplifies eq. 55 into a linear stochastic differential equation which is straight-forward to analyze.

Using this approach, all the three noise sources can be regarded as additive and we can solve the associated linear stochastic membrane equation and obtain expressions for the spectra and variance of the voltage fluctuations in closed form. We show in the companion paper that we can also apply a similar calculus when the noise sources are distributed in complex one-dimensional neuronal cable structures. This allows us to estimate the information transmission properties of linear cables under a signal detection and a signal reconstruction framework. We have reported elsewhere how these two paradigms can be exploited to characterize the capacity of simple model of an unreliable and noisy synapse (Manwani & Koch, 1998). The validity of these theoretical results need

to be assessed by comparison with experimental data from a well-characterized neurobiological system. We are currently engaged in such a quantitative comparison involving neocortical pyramidal cells (Manwani *et al.*, 1998).

Acknowledgments

This research was supported by NSF, NIMH and the Sloan Center for Theoretical Neuroscience. We thank Idan Segev, Yosef Yarom and Elad Schneidman for their comments and suggestions and Harold Lecar and Fabrizio Gabbiani for illuminating discussions.

Appendix 1. List of symbols

Symbol	Description	Dimension
γ_K	Single potassium channel conductance	pS
γ_{Na}	Single sodium channel conductance	pS
γ_L	Single leak channel conductance	pS
η_K	Potassium channel density	channels/μm^2 (patch)
		channels/μm (cable)
η_{Na}	Sodium channel density	channels/μm^2 (patch)
		channels/μm (cable)
η_{Syn}	Synaptic density	synapses/μm^2 (patch)
		synapses/μm (cable)
λ	Steady-state electrotonic space constant	μm
λ_n	Spontaneous background activity	Hz
σ_s	Standard deviation of injected current	pA
σ_V	Standard deviation of voltage noise	mV
θ_h	Time constant of sodium inactivation	msec
θ_m	Time constant of sodium activation	msec
θ_n	Time constant of potassium activation	msec
τ, τ_m	Membrane time constant	msec
ξ	Normalized coding fraction	1
A	Patch area	μm^2
B_s	Bandwidth of injected current	Hz
c_m	Specific membrane conductance per unit length	F/μm
C	Total membrane capacitance	F
C_m	Specific membrane capacitance	μF/cm^2
C_{IK}	Autocorrelation of potassium current noise	A^2/μm^2 (patch)
		A^2/μm (cable)
C_{INa}	Autocorrelation of sodium current noise	A^2/μm^2 (patch)
		A^2/μm (cable)
C_{ISyn}	Autocorrelation of synaptic current noise	A^2/μm^2 (patch)
		A^2/μm (cable)

Symbol	Description	Dimension
d	Cable diameter	μm
E_K	Potassium reversal potential	mV
E_{Na}	Sodium reversal potential	mV
E_L	Leak reversal potential	mV
E_{Syn}	Synaptic reversal potential	mV
g_K	Potassium conductance	S
g_L	Leak conductance	S
g_{peak}	Peak synaptic conductance change	pS
g_{Na}	Sodium conductance	S
g_{Syn}	Synaptic conductance	S
G	Total membrane conductance	S (patch)
		S/μm (cable)
h_∞	Steady-state sodium inactivation	1
$I(S;D)$	Mutual information for signal detection	bits
$I(I_s,V)$	Information rate for signal estimation	bits/sec
m_∞	Steady-state sodium activation	1
n_∞	Steady-state potassium inactivation	1
N_{syn}	Number of synapses activated by a pre-synaptic spike	1
P_e	Probability of error in signal detection	1
r_a	Intracellular resistance per unit length	Ω/μm
R_i	Intracellular resistivity	Ωcm
R_m	Specific leak or membrane resistance	Ωcm^2
S_{IK}	Power spectral density of potassium current noise	A^2/Hz μm^2 (patch)
		A^2/Hz μm (cable)
S_{INa}	Power spectral density of sodium current noise	A^2/Hz μm^2 (patch)
		A^2/Hz μm (cable)
S_{ISyn}	Power spectral density of synaptic current noise	A^2/Hz μm^2 (patch)
		A^2/Hz μm (cable)
S_{ITh}	Power spectral density of thermal current noise	A^2/Hz μm^2 (patch)
		A^2/Hz μm (cable)
S_V	Power spectral density of membrane voltage noise	V^2/Hz (patch)
		V^2/Hz μm (cable)
t	Time	msec
t_{peak}	Time-to-peak for synaptic conductance	msec
T	Normalized time (t/τ)	1
V	Membrane potential relative to V_{rest}	mV
V_m	Membrane potential	mV
V_{rest}	Resting potential	mV
x, y	Position	μm
X	Normalized distance (x/λ)	1

References

Abbott, L. F., Varela, J. A., Sen, K., & Nelson, S. B. 1997. Synaptic depression and cortical gain-control. *Science*, **275**, 220–224.

Bernander, O., Douglas, R., Martin, K.A.C., & Koch, C. 1991. Synaptic background activity influences spatiotemporal integration in single pyramidal cells. *Proc. Natl. Acad. Sci. USA*, **88**, 11569–11573.

Bernander, O., Koch, C., & Douglas, R. J. 1994. Amplification and linearization of distal synaptic input to cortical pyramidal cells. *J. Neurophysiol.*, **72**, 2743–2753.

Bialek, W., & Rieke, F. 1992. Reliability and information-transmission in spiking neurons. *Trends Neurosci.*, **15**, 428–434.

Bialek, W., Rieke, F., van Steveninck, R. R. D., & Warland, D. 1991. Reading a neural code. *Science*, **252**, 1854–1857.

Chow, C., & White, J. 1996. Spontaneous action potentials due to channel fluctuations. *Biophys. J.*, **71**, 3013–3021.

Clay, J. R., & DeFelice, L. J. 1983. Relationship between membrane excitability and single channel open- close kinetics. *Biophys. J.*, **42**, 151–157.

Clay, J. R., & Shlesinger, M. F. 1977. Unified theory of 1/f and conductance noise in nerve membrane. *J. Theor. Biol.*, **66**, 763–773.

Cook, E. P., & Johnston, D. 1997. Active dendrites reduce location-dependent variability of synaptic input trains. *J. .Neurophysiol.*, **78**, 2116–2128.

DeFelice, L. J. 1981. *Introduction to Membrane Noise*. Plenum Press: New York, New York.

DeFelice, L. J., & Isaac, A. 1992. Chaotic states in a random world. *J. Stat. Phys.*, **70**, 339–352.

Destexhe, A., Mainen, Z. F., & Sejnowski, T. J. 1994. Synthesis of models for excitable membranes, synaptic transmission and neuromodulation using a common kinetic formalism. *J. Comput. Neurosci.*, **1**, 195–230.

Frehland, E. 1982. *Stochastic Transport Processes in Discrete Biological Systems*. Springer-Verlag: Berlin.

Frehland, E., & Faulhaber, K. H. 1980. Nonequilibrium ion transport through pores. The influence of barrier structures on current fluctuations, transient phenomena and admittance. *Biophys. Struct. Mech.*, **7**, 1–16.

Gabbiani, F. 1996. Coding of time-varying signals in spike trains of linear and half-wave rectifying neurons. *Network: Comput. Neural Syst.*, **7**, 61–85.

Hille, B. 1992. *Ionic Channels of Excitable Membranes*. Sinauer Associates: Sunderland, Massachusetts.

Hodgkin, A. L., & Huxley, A. F. 1952. A quantitative description of membrane current and its application to conductation and excitation in nerve. *J. Physiol. (Lond.)*, **117**, 500–544.

Hoffman, D. A., & Johnston, D. 1998. Downregulation of transient K+ channels in dendrites of hippocampal CA1 pyramidal neurons by activation of PKA and PKC. *J. Neurosci.*, **18**, 3521–3528.

Hoffman, D. A., Magee, J. C., Colbert, C. M., & Johnston, D. 1997. K^+ channel regulation of signal propagation in dendrites of hippocampal pyramidal neurons. *Nature*, **387**, 869–875.

Huguenard, J. R., Hamill, O. P., & Prince, D. A. 1989. Sodium channels in dendrites of rat cortical pyramidal neurons. *Proc. Natl. Acad. Sci. USA*, **86**, 2473–2477.

Johnson, J. B. 1928. Thermal agitation of electricity in conductors. *Phys. Rev.*, **32**, 97–109.

Johnston, D., & Wu, S. M. 1995. *Foundations of Cellular Neurophysiology*. MIT Press: Cambridge, Massachusetts.

Koch, C. 1984. Cable theory in neurons with active, linearized membranes. *Biol. Cybern.*, **50**, 15–33.

Koch, C. 1999. *Biophysics of Computation: Information Processing in Single Neurons*. Oxford University Press, New York, New York.

Larsson, H.P., Kleene, S.J., & Lecar, H. 1997. Noise analysis of ion channels in non-space-clamped cables: Estimates of channel parameters in olfactory cilia. *Biophys. J.*, **72**, 1193–1203.

MacKay, D., & McCulloch, W. S. 1952. The limiting information capacity of a neuronal link. *Bull. Math. Biophys.*, **14**, 127–135.

Magee, J., Hoffman, D., Colbert, C., & Johnston, D. 1998. Electrical and calcium signaling in dendrites of hippocampal pyramidal neurons. *Ann. Rev. Physiol.*, **60**, 327–346.

Mainen, Z. F., & Sejnowski, T. J. 1998. Modeling active dendritic processes in pyramidal neurons. *In:* Koch, C., & Segev, I. (eds), *Methods in Neuronal Modeling*, second edn. pp. 171-210. MIT Pess: Cambridge, Massachusetts.

Mainen, Z. F., Joerges, J., Huguenard, J. R., & Sejnowski, T. J. 1995. A model of spike initiation in neocortical pyramidal neurons. *Neuron*, **15**, 1427–1439.

Major, G., Larkman, A. U., Jonas, P., Sakmann, B., & Jack, J. J. 1994. Detailed passive cable models of whole-cell recorded CA3 pyramidal neurons in rat hippocampal slices. *J. Neurosci.*, **14**, 4613–46 38.

Manwani, A., & Koch, C. 1998. Synaptic transmission: An information-theoretic perspective. *In:* Jordan, M., Kearns, M. S., & Solla, S. A. (eds), *Advances in Neural Information Processing Systems 10.* pp 201-207. MIT Press: Cambridge, Massachusetts.

Manwani, A., & Koch, C. 1999. Detecting and estimating signals in noisy cable structures: II. Information-theoretic analysis. *Neural Comput.*, **11**, 1831–1873.

Manwani, A., Segev, I., Yarom, Y., & Koch, C. 1998. Neuronal noise sources in membrane patches and linear cables: An analytical and experimental study. *In: Soc. Neurosci. Abstr.* #719.4, pp. 1813.

Mauro, A., Conti, F., Dodge, F., & Schor, R. 1970. Subthreshold behavior and phenomenological impedance of the squid giant axon. *J. Gen. Physiol.*, **55**, 497–523.

Mauro, A., Freeman, A. R., Cooley, J. W., & Cass, A. 1972. Propagated subthreshold oscillatory response and classical electrotonic response of squid giant axon. *Biophysik*, **8**, 118–132.

Neher, E., & Stevens, C. F. 1977. Conductance fluctuations and ionic pores in membranes. *Ann. Rev. Biophys. Bioeng.*, **6**, 345–381.

Neumcke, B. 1978. 1/f noise in membranes. *Biophys. Struct. Mech.*, **4**, 179–199.

Papoulis, A. 1991. *Probability, Random Variables, and Stochastic Processes.* McGraw-Hill: New York, New York.

Rall, W. 1967. Distinguishing theoretical synaptic potentials computed for different soma-dendritic distributions of synaptic input. *J. Neurophysiol.*, **30**, 1138–1168.

Rapp, M., Yarom, Y., & Segev, I. 1992. The impact of parallel fiber background activity on the cable properties of cerebellar Purkinje cells. *Neural Comput.*, **4**, 518–533.

Rieke, F., Warland, D., van Steveninck, R. D. R., & Bialek, W. 1997. *Spikes: Exploring the Neural Code.* MIT Press: Cambridge, Massachusetts.

Rosenfalck, P. 1969. Intra- and extracellular potential fields of active nerves and muscle fibers. *Acta Physiol. Scand. Suppl.*, **321**, 1–168.

Sabah, N. H., & Leibovic, K. N. 1969. Subthreshold oscillatory responses of the Hodgkin-Huxley cable model for the squid giant axon. *Biophys. J.*, **9**, 1206–1222.

Sabah, N. H., & Leibovic, K. N. 1972. The effect of membrane parameters on the properties of the nerve impulse. *Biophys. J.*, **12**, 1132–1144.

Schneidman, E., Freedman, B., & Segev, I. 1998. Ion-channel stochasticity may be critical in determining the reliability and precision of spike timing. *Neural Comput.*, **10**, 1679–1703.

Schwindt, P., & Crill, W. 1995. Amplification of synaptic current by persistent sodium conductance in apical dendrite of neocortical neurons. *J. Neurophysiol.*, **74**, 2220–2224.

Skaugen, E. 1980. Firing behavior in stochastic nerve membrane models with different pore densities. *Acta Physiol. Scand.*, **108**, 49–60.

Skaugen, E., & Wallœ, L. 1979. Firing behavior in a stochastic nerve membrane model based upon the Hodgkin-Huxley equations. *Acta Physiol. Scand.*, **107**, 343–363.

Spruston, N., Jaffe, D. B., & Johnston, D. 1994. Dendritic attenuation of synaptic potentials and currents: the role of passive membrane properties. *Trends Neurosci.*, **17**, 161–166.

Strassberg, A. F., & DeFelice, L. J. 1993. Limitations of the Hodgkin-Huxley formalism: effect of single channel kinetics on transmembrane voltage dynamics. *Neural Comput.*, **5**, 843–855.

Strong, S. P., Koberle, R., van Steveninck, R. D. R., & Bialek, W. 1998. Entropy and information in neural spike trains. *Phys. Rev. Lett.*, **80**, 197–200.

Stuart, G., & Sakmann, B. 1995. Amplification of epsps by axosomatic sodium channels in neocortical pyramidal neurons. *Neuron*, **15**, 1065–1076.

Stuart, G., & Spruston, N. 1998. Determinants of voltage attenuation in neocortical pyramidal neuron dendrites. *J. Neurosci.*, **18**, 3501–3510.

Stuart, G. J., & Sakmann, B. 1994. Active propagation of somatic action potentials into neocortical pyramidal cell dendrites. *Nature*, **367**, 69–72.

Theunissen, F. E., & Miller, J. P. 1991. Representation of sensory information in the cricket cercal sensory system II: Information theoretic calculation of system accuracy and optimal tuning-curve widths of four primary interneurons. *J. Neurophysiol.*, **66**, 1690–1703.

Traynelis, S. F., & Jaramillo, F. 1998. Getting the most out of noise in the central nervous system. *Trends Neurosci.*, **21**, 137–145.

Tsodyks, M. V., & Markram, H. 1997. The neural code between neocortical pyramidal neurons depends on neurotransmitter release probability. *Proc. Natl. Acad. Sci. USA*, **94**, 719–723.

Tuckwell, H. C., & Wan, F. Y. 1980. The response of a nerve cylinder to spatially distributed white noise inputs. *J. Theor. Biol.*, **87**, 275–295.

Verveen, A. A., & DeFelice, L. J. 1974. Membrane noise. *Prog. Biophys. Mol. Biol.*, **28**, 189–265.

White, J. A., Budde, T., & Kay, A. R. 1995. A bifurcation analysis of neuronal subthreshold oscillations. *Biophys. J.*, **69**, 1203–1217.

Wiener, N. 1949. *Extrapolation, Interpolation and Smoothing of Stationary Time Series.* MIT Press: Cambridge, Massachusetts.